1/16/70
8

AEC RESEARCH AND DEVELOPMENT REPORT

MASTER

1168

Y-1701
Engineering and Equipment

unclass
Kahn 1/12/70

EXPERIMENTAL AND THEORETICAL DETERMINATION OF RESIDUAL STRESSES IN FILAMENT-WOUND RINGS

B. R. Dewey
C. E. Knight, Jr.

UNION CARBIDE CORPORATION
NUCLEAR DIVISION
OAK RIDGE Y-12 PLANT

operated for the ATOMIC ENERGY COMMISSION under U. S. GOVERNMENT Contract W-7405 eng 26

UNION CARBIDE

OAK RIDGE Y-12 PLANT
P. O. Box Y
OAK RIDGE, TENNESSEE 37830

Printed in the United States of America. Available from Clearinghouse for Federal
Scientific and Technical Information, National Bureau of Standards,
U.S. Department of Commerce, Springfield, Virginia 22151
Price: Printed Copy \$3.00; Microfiche \$0.65

Date Issued: January 6, 1970

Document Y-1701

TID-4500

UNION CARBIDE CORPORATION
Nuclear Division

Y-12 PLANT

Contract W-7405-eng-26
With the US Atomic Energy Commission

EXPERIMENTAL AND THEORETICAL DETERMINATION OF RESIDUAL STRESSES IN FILAMENT-WOUND RINGS

B. R. Dewey
C. E. Knight, Jr.

Oak Ridge, Tennessee

Document Y-1701

TID-4500

DISTRIBUTION

Atomic Energy Commission

Keller, C. A.

Lawrence Radiation Laboratory

Williams, A. W.

Oak Ridge Gaseous Diffusion Plant

Jordan, R. G.
Wilcox, W. J., Jr.

Paducah Gaseous Diffusion Plant

Winkel, R. A.

Sandia-Albuquerque

Frye, E. R.

Sandia-Livermore

Loll, M. B.

The University of Tennessee

Dewey, B. R. (25)

Y-12 Plant

Ballenger, H. F. (2)
Bernander, N. K.
Burkhart, L. E.
Choat, E. E.
Cook, J. L.
Dritt, W. S.
Ebert, J. W.
Ellingson, R. D.
Evans, G. W.
Foulk, D. L.
Gritzner, V. B.
Haeusler, K. R.
Hemphill, L. F.
Hensley, C. E.
Huddleston, R. L.
Kahl, K. G.
Keith, Alvin
Knight, C. E. (25)
McLendon, J. D.
Mitchel, G. W.
Oliphant, G. W.
Perry, A. E.
Phillips, L. R.
Smith, R. D.
Stoner, H. H.
Thompson, C. H.
Tilson, F. V.
Trotter, T. C.
Warner, J. F.
Waters, J. L.
Wesley, R. L.
Yaggi, W. J.
Y-12 Central Files (5)
Y-12 Central Files (route)
Y-12 Central Files (Y-12RC)

In addition, this report is distributed in accordance with the category Engineering and Equipment, as given in the "USAEC Standard Distribution Lists for Unclassified Scientific and Technical Reports", TID-4500.

ABSTRACT

Analytical and experimental techniques have been developed and evaluated for determining residual stresses in filament-wound rings. Extension to more complex geometries appears obvious but was not investigated. These techniques should provide the tools for optimizing structural performance in filament-wound composites. All techniques proved to be useful and differed only in the accuracy of results (least accurate within ten percent; most accurate within one percent). Radial variation of material properties was accounted for in a stepwise fashion in the most accurate technique.

CONTENTS

SUMMARY

Two analytical and two experimental techniques have been developed at the Oak Ridge Y-12 Plant[a] to aid in the study of residual stresses in filament-wound rings. The state of residual stress in a ring is assumed to be one of pure bending since the ring is free from external loads. A theory-of-elasticity solution and a curved-beam solution were derived for the ring under pure bending. Both of these solutions included effects due to material-property variation through the thickness. For the range of practical interest, the curved-beam solution was within 1.5 percent of the exact-elasticity solution. Two experimental approaches were provided for acquiring data: surface-mounted strain gages and ring-diameter changes due to cutting of the rings. Both methods worked well, but the strain gages were more accurate, possibly because of measurement errors in the diameter-change method. The diameter-change method with the curved-beam solution appears to be a simple approach to evaluating, with reasonable accuracy, a quantity of specimens.

(a) Operated by Union Carbide Corporation-Nuclear Division for the US Atomic Energy Commission.

INTRODUCTION

Of the materials available today, composites are rapidly achieving recognition as the type possessing the highest performance rating. High-strength, fiber-reinforced plastics are the most frequently used composites and are best in terms of their strength-to-weight ratio. One process for making these composites is filament winding. In this process, continuous filaments are wound onto a mandrel under an applied tension (stress) with the plastic resin. This stress is "locked in" the structure after curing and produces some residual stress distribution. Although most conventional filament winding is done at a constant tension level, the resulting stress distribution is not uniform because of interactions between the layers already wound and the layer being wound. This study attempts to establish a method by which the residual stress can be determined and to ascertain some of the process parameters which control the residual stress.

Residual stresses in cylinders were studied by Mesnager(1) in 1919 and Sachs(2) in 1927. Their work involved successive boring out of material from the inner surface and measuring the outer-surface strains. The elastic equations for an isotropic, internally pressurized cylinder were used to calculate the stress in the removed material. Olson and Bert(3) expanded the Mesnager-Sachs boring-out method to cover cylindrically orthotropic materials. While this method is, in the limit, an exact solution for the residual, it is quite tedious and difficult to get accurate results.

The approach taken here can be classified as a "discrete-element" method whereby the filament-wound rings are subdivided into a plurality of separate rings. These separate rings (discrete elements) are fitted together by conditions placed on the contact pressure between rings and the displacement of adjacent points. The individual elements may be treated through an elasticity approach such as the one partially developed by Fourney,(4) or the discrete elements may be handled through the simplified curved-beam equations. For actual rings encountered in this work, both theoretical approaches give good results.

It should be noted that the residual-stress distribution is assumed to be that which results from internal pressure (due to the mandrel) and pure bending. While other factors may also influence the residual stress, this approach is felt to be representative since two conditions of force equilibrium on an element in the "free" state which must be satisfied are: net force equal to zero and net moment equal to zero. This approach also allows a more general type of structure to be analyzed since the element can be taken from any fabricated shape, and material properties may vary arbitrarily through the cross section. The experimental work reported herein tends to confirm the validity of this method for determining residual stresses.

THIS PAGE

WAS INTENTIONALLY

LEFT BLANK

DETERMINATION OF RESIDUAL STRESSES

ANALYSIS BY THE ELASTICITY THEORY

In the solution for the stress, strain, and displacement relations of an elastic body, it is necessary to satisfy the conditions of equilibrium, compatibility, and the constitutive equation; ie, Hooke's law. The basic procedures for anisotropic rings are outlined in Chapter 3 of the text by Lekhnitskii.[5] Solutions in closed form are available for only a limited class of problems, generally problems which possess a large degree of symmetry. Analysis of the residual strain in a filament-wound ring has a solution in closed form[4] provided there is an axially symmetric state of stress, the material is uniform, and there is cylindrical anisotropy. Through the fitting together of separate solutions for uniform material, it is possible to analyze a ring of nonuniform material where the nonuniformity is taken in successive discrete layers. This technique is known as the discrete-element method.

Single-Layer Ring

First consider the axially symmetric ring of uniform material with coordinates and dimensions as shown in Figure 1. It is assumed that all the residual stress is "unlocked" when a radial cut is made in the ring. It is further assumed that the residual stress is axially symmetric and that this residual stress is numerically equal to the pure flexural stress necessary to restore a cut ring to its original configuration.

The equations of equilibrium[6] for this state of stress reduce to:

$$\frac{\partial \sigma_r}{\partial r} + \frac{1}{r}\frac{\partial \tau_{r\theta}}{\partial \theta} + \frac{\sigma_r - \sigma_\theta}{r} + R = 0, \text{ and} \tag{1}$$

$$\frac{1}{r}\frac{\partial \sigma_\theta}{\partial \theta} + \frac{\partial \tau_{r\theta}}{\partial r} + \frac{2}{r}\tau_{r\theta} = 0. \tag{2}$$

Due to the axial symmetry, $\partial\sigma_\theta/\partial\theta = 0$ and Equation 2 further reduces to:

$$\frac{d\tau_{r\theta}}{dr} + \frac{2}{r}\tau_{r\theta} = 0. \tag{3}$$

Integration of Equation 3 (variables separable) yields the result that:

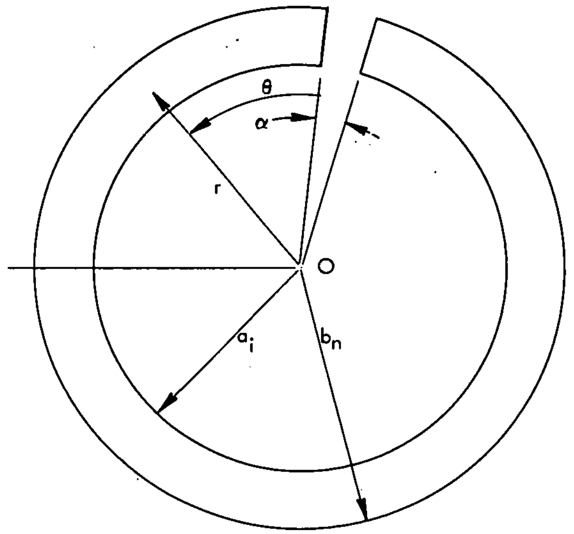

Figure 1. COORDINATES AND DIMENSIONS OF AN AXIALLY SYMMETRIC CUT RING. (The Origin of Coordinates is Fixed at O)

$$\tau_{r\theta} = K/r^2,$$

where K is a constant of integration. However, $\tau_{r\theta}$ equals zero at the inner and outer surfaces of the ring, which forces K to be identically zero. Hence, $\tau_{r\theta}$ equals zero everywhere in the ring, which is the expected result. As a consequence, Equation 1 further reduces to:

$$\sigma_\theta = \sigma_r + r\frac{d\sigma_r}{dr} \tag{4}$$

in the absence of a body force (R = 0).

For the axially symmetric state of stress, with the restriction that second-order terms in the strain tensor are negligible, the strain-displacement equations(6) reduce to:

$$\epsilon_r = du/dr, \text{ and} \tag{5}$$

$$\epsilon_\theta = \frac{u}{r} + \frac{1}{r}\frac{\partial v}{\partial \theta}. \tag{6}$$

Similarly, the compatibility equation[6] states that:

$$\frac{1}{r}\frac{d\epsilon_r}{dr} - \frac{2}{r}\frac{d\epsilon_\theta}{dr} - \frac{d^2\epsilon_\theta}{dr^2} = 0. \tag{7}$$

The appropriate elastic constants for the cylindrically anisotropic state of plane stress are:[5] E, E', ν, and ν'.[b] The generalized Hooke's law[5] for these conditions reduces to:

$$\epsilon_r = \sigma_r/E' - \nu\sigma_\theta/E, \text{ and} \tag{8}$$

$$\epsilon_\theta = \sigma_\theta/E - \nu'\sigma_r/E'. \tag{9}$$

Substitution of Equations 8, 9, and 4 into Equation 7 yields the ordinary differential equation:

$$\frac{1}{r}\frac{d}{dr}\left[\frac{\sigma_r}{E'} - \frac{\nu\sigma_r}{E} - \frac{\nu r}{E}\frac{d\sigma_r}{dr}\right] - \frac{2}{r}\frac{d}{dr}\left[\frac{\sigma_r}{E} + \frac{r}{E}\frac{d\sigma_r}{dr} - \frac{\nu'}{E'}\sigma_r\right]$$
$$- \frac{d^2}{dr^2}\left[\frac{\sigma_r}{E} + \frac{r}{E}\frac{d\sigma_r}{dr} - \frac{\nu'}{E'}\sigma_r\right] = 0. \tag{10}$$

The general solution of Equation 10 is:

$$\sigma_r = A + Br^{-(k+1)} + Cr^{k-1}, \tag{11}$$

and Equations 11 and 4 yield immediately:

$$\sigma_\theta = A - Bkr^{-(k+1)} + Ckr^{k-1}, \tag{12}$$

where:

$$k^2 = E/E' = \nu/\nu'. \tag{13}$$

Substituting Equations 11 and 12 into Equation 8 yields an expression for ϵ_r in terms of three constants: A, B, and C. Next, substituting this expression for ϵ_r into Equation 5 and integrating gives:

(b) In other notations, $E = E_\theta$, $E' = E_r$, $\nu = \nu_{\theta r}$, and $\nu' = \nu_{r\theta}$.

$$u = \frac{1}{E}\left[(k^2 - \nu)rA - (k + \nu)r^{-k}B + (k - \nu)r^{k}C\right]. \tag{14}$$

In a similar fashion, Equation 6 yields an expression for "u" directly:

$$u = \frac{1}{E}\left[(1 - \nu)rA - (k + \nu)r^{-k}B + (k - \nu)r^{k}C\right] - \frac{\partial v}{\partial \theta}. \tag{15}$$

When Equations 14 and 15 are equated, it is found that:

$$\frac{\partial v}{\partial \theta} = \frac{1 - k^2}{E} rA. \tag{16}$$

Upon integrating Equation 16 with the use of Equation 13:

$$v = (1/E - 1/E')r\theta A, \tag{17}$$

where some f(r) derived in the integration is identically zero by the choice of "v" as zero at $\theta = 0$.

Evaluation of the constants (A, B, and C) depends upon the manner in which the input data are obtained from the ring before and after cutting.

<u>Diameter Change of the Ring as Input</u> - Consider the cut ring of Figure 1. To close the small gap, α:

$$v = \alpha r \tag{18}$$

at $\theta = 2\pi$. By Equation 17, then:

$$A = \frac{\alpha}{2\,(1/E - 1/E')}. \tag{19}$$

The term "α" may be approximated by the expression:

$$\alpha = \frac{2\pi(a^* - a)}{a}, \tag{20}$$

where "a" represents the inner radius of the ring before cutting and "a^*" the radius after cutting. Hence:

$$A = \frac{a^* - a}{a(1/E - 1/E')}. \tag{21}$$

At the inner and outer boundaries, $\sigma_r(a) = \sigma_r(b) = 0$. Thus, from Equation 11:

$$B = A \frac{b^{k-1} - a^{k-1}}{a^{k-1}b^{-k-1} - b^{k-1}a^{-k-1}}, \text{ and} \tag{22}$$

$$C = -A \frac{b^{-k-1} - a^{-k-1}}{a^{k-1}b^{-k-1} - b^{k-1}a^{-k-1}} . \tag{23}$$

Furthermore, at the outer and inner boundaries, Equation 9 reduces to $\epsilon_\theta = \sigma_\theta/E$. The strains on these surfaces are thus:

$$\epsilon_o = \frac{A}{E} - \frac{B}{E} kb^{-k-1} + \frac{C}{E} kb^{k-1}, \text{ and} \tag{24}$$

$$\epsilon_i = \frac{A}{E} - \frac{B}{E} ka^{-k-1} + \frac{C}{E} ka^{k-1}, \tag{25}$$

where A, B, and C are found as described previously.

Then substitution of Equations 21 through 23 into Equations 11 and 12 yields the residual stress distribution in the ring prior to cutting.

Strain Change on the Surface as Input - If a strain gage is mounted on the surface prior to making the radial cut, the change in strain after the cut is made is the amount of residual strain relief. If the strain gage is mounted on the inner surface and the change in strain is ϵ_i, Equations 22, 23, and 25 uniquely determine A, thus:

$$A = \frac{E\,\epsilon_i}{\left[1 - k \dfrac{b^{k-1}a^{-k-1} - 2a^{-2} + b^{-k-1}a^{k-1}}{a^{k-1}b^{-k-1} - b^{k-1}a^{-k-1}}\right]} . \tag{26}$$

Now, as before, the values of B and C are given by Equations 22 and 23, and the value of ϵ_o is given by Equation 24. If the strain is measured on the outer surface, the derivation would proceed in a similar manner.

The computer program for the foregoing theory is described in the Appendix (Page 35).

Multilayer Ring

A nonuniform distribution of fibers in the radial direction causes a corresponding variation of the elastic properties in the radial direction. Such a case is of practical interest because a nonuniform distribution of fibers is inevitable in the winding process since there is a natural tendency for resin to be squeezed outward. Alternatively, a nonuniform distribution of fibers in the radial direction may be introduced intentionally to alter the characteristics of the ring.

The nonuniformity of the material is observed experimentally from an analysis of samples cut from layers of finite thickness. Such samples are reduced by burning off the resin which permits determination of the weight ratio of resin to fiber. Elastic properties as a function of the resin-to-fiber ratio have been determined empirically. Hence, the distribution of the elastic properties in the radial direction may be found for any number, n, of discrete steps. By fitting together elasticity equations based on uniform material for the "n" discrete layers by means of the appropriate boundary conditions, it is possible to solve for the stresses, strains, and displacements in the multilayered ring.

By denoting a_1 as the inner radius of the first layer, b_1 as the outer radius of the first layer, a_i as the inner radius of the ith layer, . . ., the results of the previous section which are pertinent to this analysis can be rewritten as given in the treatment that follows.

Stresses from Equations 11 and 12:

$$\sigma_r = A_i + B_i r^{k_i - 1} + C_i r^{k_i - 1}, \text{ and} \tag{27}$$

$$\sigma_\theta = A_i - B_i r^{k_i - 1} + C_i k_i r^{k_i - 1}. \tag{28}$$

Displacements from Equations 14 and 17:

$$u = \frac{1}{E_i}\left[(k_i^2 - \nu_i) r A_i - (k_i + \nu_i) r^{-k_i} B_i + (k_i - \nu_i) r^{k_i} C_i\right], \text{ and} \tag{29}$$

$$v = \left[\frac{1}{E_i} - \frac{1}{E_i'}\right] r\theta A_i. \tag{30}$$

The discrete layers are matched by boundary conditions which depend on whether the input data are from a diameter-change measurement or a surface-strain measurement.

Diameter Change of the Ring as Input - The constant, A_i, is determined through the use of Equation 21 at the inner surface of the composite ring. Thus:

$$A_i = \frac{a_1^* - a_1}{a_1\left[\frac{1}{E_i} - \frac{1}{E_i'}\right]} . \tag{31}$$

It is noted that Equation 30, which is the tangential displacement, v, is an expression for the size of the gap of the cut ring.

The remaining (3n-1) constants, A_i, B_i, and C_i, are determined from conditions placed on the stresses and displacements. At the inner and outer surfaces, the radial component of stress is zero, or:

$$\sigma_r(a_1) = \sigma_r(b_n) = 0. \tag{32}$$

Between the "n" discrete layers of the nonuniform ring, the radial component of stress and both components of the displacement must match. Thus:

$$\sigma_r(b_{i-1}) = \sigma_r(a_i), \tag{33}$$

$$u(b_{i-1}) = u(a_i), \text{ and} \tag{34}$$

$$v(b_{i-1}) = v(a_i). \tag{35}$$

The matrix representing this system of equations is shown in Figure 2.

Once the constants A_i, B_i, C_i are computed, the strain distribution can be computed by a modification of Equations 24 or 25:

$$\epsilon(r) = \frac{A_i}{E_i} - \frac{B_i}{E_i} k_i r^{-k_i-1} + \frac{C_i}{E_i} k_i r^{k_i-1} . \tag{36}$$

Note that $\epsilon(r)$ is not a continuous function from one layer to the next through the ring. The angle, α, which measures the gap (Figure 1) can be computed by Equation 20 as before, with any consistent radii used for "a" and "a*".

<u>Strain Change on the Surface as Input</u> - The solution for the constants A_i, B_i, and C_i involves 3n simultaneous equations when a change in the surface strain is given as input data.

If, for example, the strain is measured on the inner surface, one equation follows from Equation 36 with $r = a_1$, or:

$$\frac{1}{E_1} A_1 - \frac{k_1 a_1^{-k_1 - 1}}{E_1} B_1 + \frac{k_1 a_1^{k_1 - 1}}{E_1} C_1 = \epsilon_i \, . \tag{37}$$

Two additional equations result from zero radial stress on the inner and outer surfaces, namely:

$$\sigma_r(a_1) = 0, \text{ and} \tag{38}$$

$$\sigma_r(b_n) = 0. \tag{39}$$

The remaining (3n-3) equations result from matching radial stress, radial displacement, and transverse displacement at the interfaces between the layers, thus:

$$\sigma_r(b_{i-1}) = \sigma_r(a_i), \tag{40}$$

$$u(b_{i-1}) = u(a_i), \text{ and} \tag{41}$$

$$v(b_{i-1}) = v(a_i). \tag{42}$$

The matrix representation of the system of equations is given in Figure 3.

When the constants A_i, B_i, and C_i have been determined, the strain distribution can be computed as before through Equation 36 and the stress distribution through Equations 27 and 28.

The computer program involved with this section is also described in detail in the Appendix (Page 37).

$$
\begin{bmatrix}
1 & 0 & 0 & 0 & 0 & 0 & 0 & 0 & 0 & \cdots & & & & 0 \\
1 & a_1^{-k_1-1} & a_1^{k_1-1} & 0 & 0 & 0 & 0 & 0 & 0 & \cdots & & & & 0 \\
1 & b_1^{-k_1-1} & b_1^{k_1-1} & -1 & -a_2^{-k_2-1} & -a_2^{k_2-1} & 0 & 0 & 0 & \cdots & & & & 0 \\
\frac{(k_1^2-\nu_1)b_1}{E_1} & \frac{-(k_1+\nu_1)b_1^{-k_1}}{E_1} & \frac{(k_1-\nu_1)b_1^{k_1}}{E_1} & \frac{-(k_2^2-\nu_2)a_2}{E_2} & \frac{(k_2+\nu_2)a_2^{-k_2}}{E_2} & \frac{-(k_2-\nu_2)a_2^{k_2}}{E_2} & 0 & 0 & 0 & 0 & \cdots & & & 0 \\
\frac{1}{E_1}-\frac{1}{E_1'} & 0 & 0 & \frac{-1}{E_2}+\frac{1}{E_2'} & 0 & 0 & 0 & 0 & 0 & 0 & \cdots & & & 0 \\
0 & 0 & 0 & 1 & b_2^{-k_2-1} & b_2^{k_2-1} & -1 & -a_3^{-k_3-1} & -a_3^{k_3-1} & 0 & \cdots & & & \cdots \\
0 & 0 & 0 & \frac{(k_2^2-\nu_2)b_2}{E_2} & \frac{-(k_2+\nu_2)b_2^{-k_2}}{E_2} & \frac{(k_2-\nu_2)b_2^{k_2}}{E_2} & \frac{-(k_3^2-\nu_3)}{E_3} & \frac{(k_3+\nu_3)a_3^{-k_3}}{E_3} & \frac{-(k_3-\nu_3)a_3^{k_3}}{E_3} & 0 & \cdots & & & \\
0 & 0 & 0 & \frac{1}{E_2}-\frac{1}{E_2'} & 0 & 0 & \frac{-1}{E_3}+\frac{1}{E_3'} & 0 & 0 & 0 & \cdots & & & \\
0 & \cdots & & \cdots & & & & & & & & & & \\
\cdots & \cdots & & \cdots & & & & & & & & & & \\
0 & \cdots & & \cdots & & & & & & & & 1 & b_n^{k_n\ 1} & b_n^{k_n-1}
\end{bmatrix}
\begin{bmatrix}
A_1 \\ B_1 \\ C_1 \\ A_2 \\ B_2 \\ C_2 \\ \\ \\ \\ \\ C_n
\end{bmatrix}
=
\begin{bmatrix}
\frac{a_1^* - a_1}{a_1\left[\frac{1}{E_i}-\frac{1}{E_i'}\right]} \\ 0 \\ 0 \\ 0 \\ 0 \\ 0 \\ \\ \\ \\ \\ 0
\end{bmatrix}
$$

Figure 2. MATRIX REPRESENTATION OF EQUATIONS 32 THROUGH 35.

$$
\begin{bmatrix}
\frac{1}{E_1} & \frac{-k_1 a_1^{-k_1-1}}{E_1} & \frac{k_1 a_1^{k_1-1}}{E_1} & 0 & 0 & & & & & & \\
1 & a_1^{-k_1-1} & a_1^{k_1-1} & 0 & 0 & & & & & & \\
1 & b_1^{-k_1-1} & b_1^{k_1-1} & -1 & -a_2^{-k_2-1} & a_2^{k_2-1} & & & & & \\
\frac{(k_1^2-\nu_1)b_1}{E_1} & \frac{-(k_1+\nu_1)b_1^{-k_1}}{E_1} & \frac{(k_- - \nu_1)b_1^{k_1}}{E_1} & \frac{-(k_2^2-\nu_2)a_2}{E_2} & \frac{(k_2+\nu_2)a_2^{-k_2}}{E_2} & \frac{(k_2-\nu_2)a_2^{k_2}}{E_2} & 0 & & & & \\
\frac{1}{E_1}-\frac{1}{E_1'} & 0 & 0 & -\frac{1}{E_2}+\frac{1}{E_2'} & 0 & 0 & 0 & 0 & & & \\
0 & 0 & 0 & 1 & b_2^{-k_2-1} & b_2^{k_2-1} & -1 & -b_2^{-k_2-1} & -b_2^{k_2-1} & \cdots & \\
0 & 0 & 0 & \frac{(k_2^2-\nu_2)b_2}{E_2} & \frac{-(k_2+\nu_2)b_2^{-k_2}}{E_2} & \cdots & & & & & \\
0 & 0 & 0 & \frac{1}{E_2}-\frac{1}{E_2'} & 0 & 0 & \frac{1}{E_3}-\frac{1}{E_3'} & \cdots & & & \\
0 & 0 & 0 & & & & & & & & \\
 & & & & & & & 0 & 1 & b_n^{-k_n-1} & b_n^{k_n-1}
\end{bmatrix}
\begin{bmatrix} A_1 \\ B_1 \\ C_1 \\ A_2 \\ B_2 \\ C_2 \\ \\ \\ B_n \\ C_n \end{bmatrix}
=
\begin{bmatrix} \epsilon_i \\ 0 \\ 0 \\ 0 \\ 0 \\ 0 \\ \\ \\ \\ 0 \end{bmatrix}
$$

Figure 3. MATRIX REPRESENTATION OF EQUATIONS 37 THROUGH 42.

ANALYSIS BY THE CURVED-BEAM THEORY

A somewhat simpler analysis than that of the elastic-theory analysis for the residual strain distribution is achieved through the use of the approximate curved-beam theory.[7] Both the analysis by the theory of elasticity and that by the curved-beam theory are based on the assumption that the residual strain is equal to the strain induced by pure bending moments applied to a radially cut ring. The pure bending moments must be of proper magnitude and sign that are just sufficient to restore the cut ring to its original configuration.

The approximate curved-beam theory assumes that the radial component of stress is zero and that only the modulus of elasticity in the circumferential direction needs to be considered in determining the elastic behavior of the ring. Variations in the material composition in the radial direction are inevitable in the winding process. Such variations may also be intentionally induced to alter the properties of the rings. Through the use of empirical data relating modulus of elasticity to the fiber-resin ratio, the modulus of elasticity may be expressed as a function of "r".

The coordinates and notations are shown in Figure 4. Here, the radius, R, locates the neutral surface; radii a_j and b_j denote the inner and outer radii, respectively, of the jth layer. The z coordinate is measured radially outward from the neutral surface. The radial and circumferential components of displacement of the point are denoted by "u" and "v". Bars ($\bar{u}$, $\bar{v}$) denote a point on the neutral surface. The elongation of an element subtended by $d\theta$ is $(R + z)\epsilon d\theta$, where "ϵ" is the circumferential strain associated with that element. The assumption that plane sections remain plane under deformation dictates that:

$$\frac{(R + z)\epsilon}{z} = \text{Constant}, \tag{43}$$

which implies a hyperbolic strain distribution:

$$\epsilon = K \frac{z}{R + z}. \tag{44}$$

The factor, K, can be interpreted from the geometry of bending as:

$$K = \frac{\bar{u}'(\theta)}{\theta}, \tag{45}$$

where "$\bar{u}'$" represents the slope of the neutral surface. For a state of pure flexure, "K" is constant since "ϵ" is a function of "z" alone.

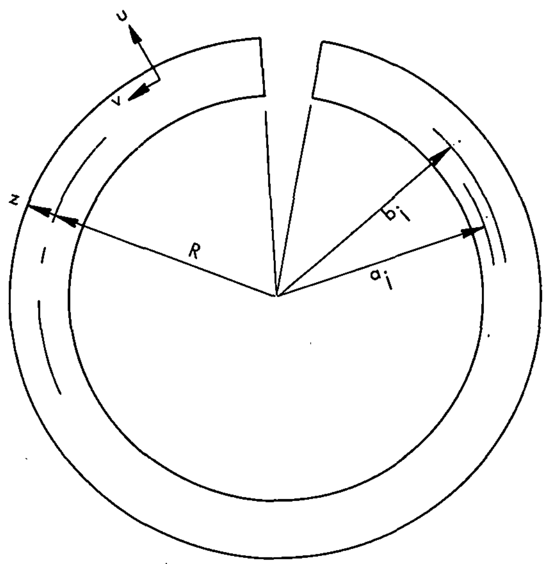

Figure 4. NOTATIONS FOR A CUT RING.

When a ring is cut and the residual stress is relieved, the angle, α (Figure 4), is given by $\bar{v}(2\pi)/R$. The distance, R, denotes the radius of curvature of the neutral surface of the ring before cutting, while "R^*" denotes the same radius after cutting. Note that "R^*" may be either greater than or less than "R", depending on the sign of the residual stress. The circumferential component of displacement at the gap, $\bar{v}(2\pi)$, is given by $R\alpha$, or:

$$\bar{v}(2\pi) = 2\pi(R^* - R). \tag{46}$$

A negative value of $\bar{v}(2\pi)$ is physically possible if two radial cuts are made in the ring. When the member is subjected to a pure bending moment to close the gap, $\bar{u}'(2\pi) = \alpha$. Thus, by Equation 45:

$$K = \frac{R^* - R}{R}. \tag{47}$$

If the circumferential modulus of elasticity is taken as any function, E(z), the stress-strain relationship $\sigma = \epsilon E(z)$ and Equation 43 yield:

$$\frac{(R + z)\sigma}{a\ E(z)} = \text{Constant}. \tag{48}$$

When Equation 48 is substituted into the equilibrium equation, $\int \sigma dA = 0$,

$$\int_A \frac{z\ E(z)}{R + z}\, dA = 0 \tag{49}$$

is obtained, which defines the location of the neutral surface.

When E(z) is a continuous function, Equation 49 may be integrated directly to find "R". However, it is more often the case that samples are taken from discrete layers through the ring. From known relationships between the fiber-to-resin ratio and the elastic modulus, the modulus can be determined for each "i" layer. Thus, Equation 49 may be rewritten:

$$\sum_{i=1}^{n} \left[E_i \int_{A_i} \frac{z}{R+z}\, dA \right] = 0. \tag{50}$$

When the "n" layers have rectangular cross sections of constant width and variable thickness, t_i, each, Equation 50 may be simplified accordingly to give:

$$\sum_{i=1}^{n} \left[E_i \left(t_i - R \ln \frac{b_i}{a_i} \right) \right]. \tag{51}$$

Rearranging Equation 51 gives an explicit expression for the location of the neutral surface, thus:

$$R = \frac{\sum_{i=1}^{n} E_i t_i}{\sum_{i=1}^{n} E_i \ln (b_i/a_i)}. \tag{52}$$

With the "R" given by Equation 52, the strain distribution may now be found from Equation 43. The constant in Equation 44 can be evaluated routinely if one of the surface strains is measured with a strain gage. Thus, if the strain, ϵ_i, is read on the inner surface, the strain on the outer surface is:

$$\epsilon_o = \frac{a(b - R)}{b(a - R)} \epsilon_i. \tag{53}$$

On the other hand, if the inside diameter is noted before and after the radial cut is made, the strain distribution follows from Equations 44 and 47. Since it has been assumed that the radial component of stress is zero, it follows that the radial component of the strain is of small order. Hence, the thickness change can be neglected and the "K" of Equation 47 is:

$$K = \frac{a_1^* - a_1}{a_1}, \tag{54}$$

where a_1 is the inside radius of the ring before cutting and a_1^* the inside radius of the ring after cutting.

COMPARISON OF THEORIES

A comparison of the results for the residual-strain distribution obtained from the elasticity theory with those obtained from the curved-beam theory is most directly done numerically. In general, it is expected that the simpler curved-beam theory should give less satisfactory results than the elasticity theory when either the ring is relatively thick (R/t small) or the anisotropy is great (as indicated by the magnitude of k, which is the square root of the ratio of E/E').

In addition, the significance of a nonuniform distribution of fibers in the radial direction is of interest. In many instances, a determination of the elastic properties at several discrete layers involves somewhat more effort than may be justified. Hence, comparisons are also made between the two theories on the basis of the differences predicted for the amount of radial variation of the elastic properties.

Comparison of the Two Theories for Uniform Material

Since the curved-beam theory assumes at the outset that the radial component of stress and strain is zero, this theory neglects any contribution of E_r (the elastic modulus in the radial direction). On the other hand, E_r is incorporated into the elasticity equations through the parameter $k = \sqrt{E_\theta/E_r}$. It is noted that the elasticity equations as they stand will not run for isotropic material ($k = 1$).(c) If isotropic material is to be considered, it is suggested that a value of E_θ, which is slightly larger than E_r, be selected so that "k" is on the order of 1.1.

For comparison of the strain distributions resulting from the two theories, it is convenient to consider the dimensionless ratio of the strain on the outer surface to that on the inner surface, ϵ_o/ϵ_i. With reference to Figure 5, it is noted that consideration of "k" is most important when the ring is relatively thick ($R/t < 5$). However, a practical range of "k" encountered is $1 < k < 3$, and it is seen in Figure 5 that the curved-beam and elasticity theories give excellent agreement within this range.

(c) The solution for isotropic material may be found in the work of Timoshenko.(6) The general solution for the stresses is of a slightly different form.

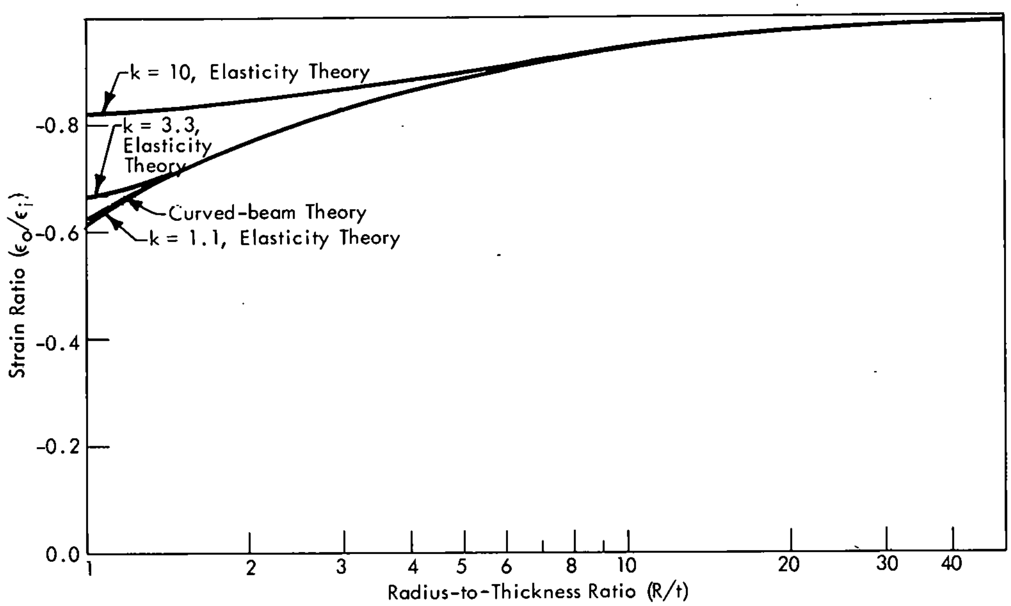

Figure 5. COMPARISON OF THE TWO THEORIES FOR THE CASES WHERE THERE IS A UNIFORM DISTRIBUTION OF FIBERS IN THE RADIAL DIRECTION.

If the rings under consideration fall within the favorable ranges of k and R/t for the curved-beam theory, the use of this theory gives the important advantage that the modulus of elasticity of the material does not have to be known to determine the residual strain distribution.

Importance of Nonuniform Material

The residual-strain distribution is a function of the material properties as well as the radius-to-thickness ratio. When there is a wide variation in the modulus of elasticity through the cross section of the ring, there can be a significant effect upon the strain distribution.

In Figure 6 are shown the results of a study run by the elasticity program for rings having four discrete layers. The circumferential modulus of elasticity was made to vary in such a way that the differences in the values of E_θ were always equal, giving a "linear" variation of E_θ in four steps. The amount of variation is thus expressed by the ratio of E_θ for the outer layer to that of E_θ for the inner layer. In this study, value of the radial elastic modulus for all layers was taken as 0.3 of the mean value of E_θ. While the range of the E_o/E_i ratio, as shown in Figure 6, is admittedly much wider than would be encountered in practice, it is still apparent that the distribution of E_θ can be important. Also, it can be seen that the effect is only slightly less pronounced for relatively thick rings (R/t = 1.25) than it is for relatively thin rings. In addition, it is noted that there are many cases, the chances for which are more likely with thin rings, in which the residual strain is greater on the outer surface than on

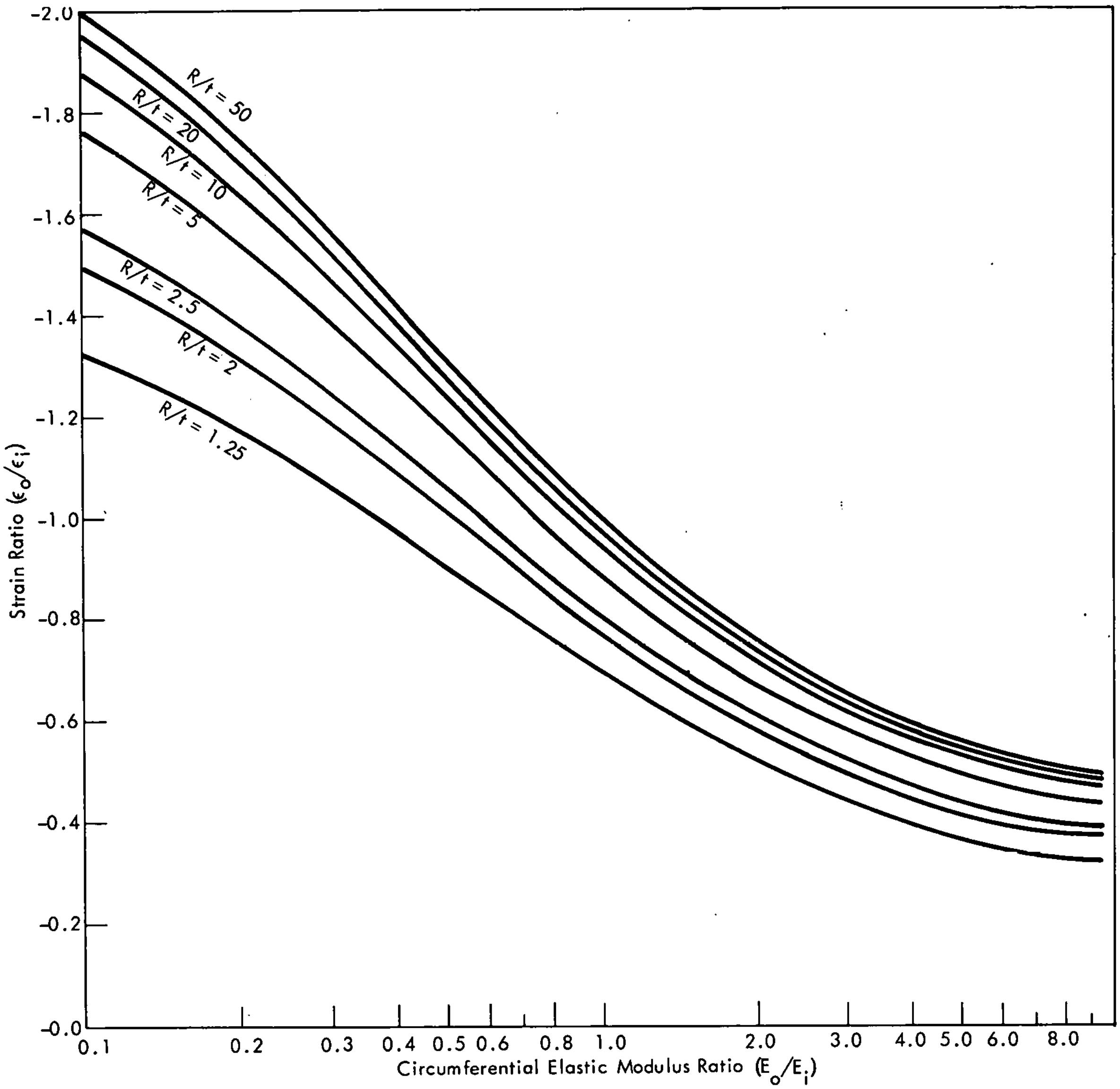

Figure 6. VARIATION OF STRAIN DISTRIBUTION WITH NONUNIFORMITY OF MATERIAL. (Four Discrete Layers, Elasticity Theory; $E_r = 0.3\ E_\theta$ Mean)

the inner surface. This seeming paradox has been observed experimentally, and is explained by the fact that the material has a lower E_θ on the outer layers.

If the value of "k" is not large, it might be expected on the basis of the previous results for uniform material that the results obtained from the elasticity theory and those obtained from the curved-beam theory would be in substantial agreement for nonuniform material. Such is the case. In Figure 7 is plotted the relative error of the curved-beam theory, which can be compared to the elasticity theory which is plotted in Figure 6.

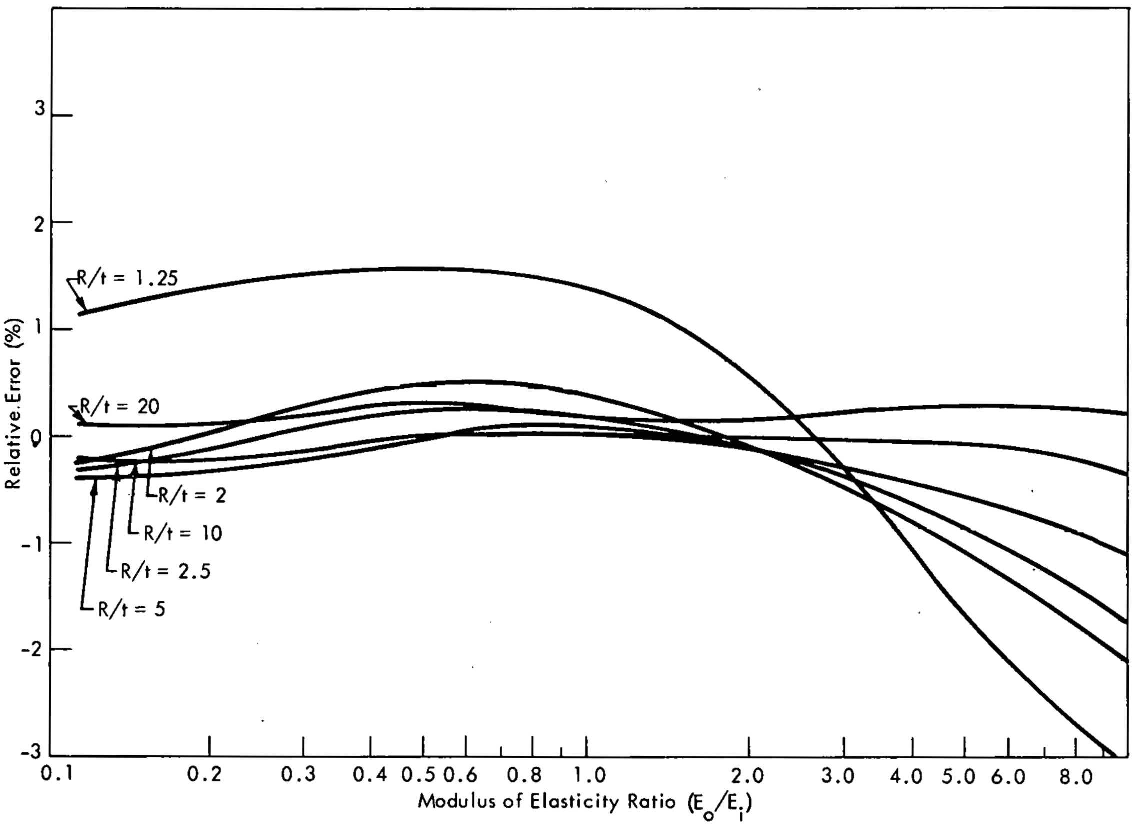

Figure 7. RELATIVE ERROR OF RESULTS FROM CURVED-BEAM THEORY COMPARED TO ELASTICITY THEORY. (E_r = 0.3 E_θ Mean; Four Discrete Layers)

For the case of a relatively thick ring (R/t = 1.25) the two theories agree within ± 1.5 percent for $0.1 < E_o/E_i < 4.5$. The agreement between the two theories improves as the rings become thinner. For R/t ≤ 2, the two theories agree within ± 0.5 percent for $0.1 < E_o/E_i < 3$. For R/t ≤ 10, the two theories agree within ± 0.3 percent for $0.1 < E_o/E_i < 10$.

EXPERIMENTAL PROCEDURE

In order to check the theory and determine methods of controlling residual strains in filament-wound rings, several cylinders were fabricated. The process was one of wet winding with single-end "S" glass yarn and a dip-type resin impregnation tank. Tension was applied before impregnation by magnetically loaded polished discs. Type ERL 2258/MPDA (100/20 pbw) epoxy resin was used as the matrix. Fiber-winding tension and resin migration were the process variables that were controlled. These variables were step incremented at quarter-thickness points. Specimens were fabricated with combinations of resin cure at quarter thicknesses, constant tension, and linear stepwise increase or decrease of tension. A total of twelve cylinders (two sets at different times) were made with three of each set given an intermediate cure and three completely wound and

Table 1

FABRICATION DATA FROM TEST SPECIMENS

Specimen Number	Number of Cure Cycles	Tension (grams)
1292-01	1	250 (constant)
1292-02	4	100 - 400
1292-03	4	250 (constant)
1292-04	4	400 - 100
1292-05	1	100 - 400
1292-06	1	400 - 100
1-1A	1	200 (constant)
1-2A	1	400 - 100
1-3A	1	100 - 400
1-4A	4	200 (constant)
1-5A	4	400 - 100
1-6A	4	100 - 400

cured. Data for the cylinders are listed in Table 1. All cylinders were wound on rigid aluminum mandrels and rotationally cured for two hours at 185° F and two hours at 300° F. From these cylinders, one-quarter-inch-wide rings were machined by diamond wheel grinding. Inner and outer surfaces were not machined.

As discussed in the topics on theoretical analysis, two techniques were used to determine residual strains: strain-gage and deflection measurements. Strain gages (micro measurements, Type EA-06-250BG-120) were applied to one ring from each of the six cylinders on the inside and outside surfaces. These gages were connected in a half-bridge arrangement using a BLH strain indicator (Model 120C). The bridges were balanced then the ring was cut. A segment was removed when the rings closed on the saw cut. The final strain-gage readings indicated the amount of residual bending strain present in the rings as fabricated. Two sets of gages were mounted on each ring and the average value for the inside and outside gages was used. As mentioned in the theoretical discussion, only one strain reading is needed for determining the residual distribution. The second reading thus provides a check on the theory. In addition to strain-gage readings, the inside-diameter change of the ring was measured. Diameters were measured and recorded before and after cutting by using an inside micrometer. This step provided another set of data for the same ring and a comparison with the strain-gage values.

In order to check the importance of material nonuniformity as well as to provide an idea of the validity of the theoretical analysis, samples were taken from each of the rings to determine their material properties. A one-half-inch-long segment of the ring was divided at quarter-thickness intervals, and a chemical analysis was made for the fiber/resin ratio and density for these sub samples. Results from the chemical analysis were used to calculate the fiber volume percent and void percent in the material. These data were used along with experimental curves to determine the tangential and radial moduli of elasticity, and in the computer programs to determine the nonuniformity effects. These results are discussed in the next topic.

EXPERIMENTAL RESULTS AND COMPARISONS

Uniform Distribution of Fibers - Strain-Gage Input

Experimental results wee obtained by Fourney[4] for five rings where a uniform distribution of fibers was assumed in the radial direction. These experimental results are compared to the elasticity and curved-beam theories in Table 2. A constant value of $E = 7.4 \times 10^6$ psi was used for the calculated values. Since the values of R/t in Table 2 range from 11.3 to 16.1, according to Figure 5, virtual agreement is expected between the elasticity and curved-beam theories, as appears to be the case here. Agreement between the experimental results (strain-gage readings only) and theoretical results is favorable, as shown in the last column of Table 2.

Table 2

COMPARISON OF STRAIN DISTRIBUTION PREDICTED BY THEORIES WITH RESULTS OBTAINED BY EXPERIMENTS FOR RINGS OF UNIFORM MATERIAL

Experimental Data[1]					Theoretical Data		
Inner Radius (in)	Average Thickness (in)	R/t	ϵ_i (μ in/in)	ϵ_o (μ in/in)	Elasticity ϵ_o (μ in/in)	Curved Beam ϵ_o (μ in/in)	Percent Difference from Experimental Results
2.68	0.2372	11.3	180	-158	-170	-170.1	+ 7.38
2.65	0.1646	16.1	140	-146	-134.5	-134.5	- 8.20
2.65	0.1837	14.4	128	-119	-122.6	-122.4	+ 2.82
2.65	0.2218	11.9	126	-108	-119	-119.4	+10.02
2.65	0.2210	12.0	152	-147	-144	-144.1	- 1.99

(1) From Fourney.[4]

Description of Test Specimens with Radial Variation of Fiber Distribution

Twelve test specimens with the winding tension varied on four discrete steps were constructed at the Y-12 Plant. Four strain gages, two inside and two outside, were mounted in the circumferential direction on the rings. Diameter and strain-gage readings were recorded before and after the radial cut was made in the rings. Subsequent chemical analysis by resin burnoff was used to determine the fiber/resin ratio. These data were then converted through the use of empirical relationships to the modulus of elasticity. A description of the twelve test rings is given in Table 3. The R/t ratios here range from 9.1 to 10.3; which, as before, is in the range where good theoretical agreement exists between the elasticity and curved-beam theories.

Table 3
DESCRIPTION OF TEST RINGS OF NONUNIFORM MATERIAL

Specimen Number	Inner Radius (in)	Average Thickness (in)	R/t	Circumferential Modulus of Elasticity(1) Layer 1 (inner) (10^6 psi)	Layer 2 (10^6 psi)	Layer 3 (10^6 psi)	Layer 4 (outer) (10^6 psi)	Measured Strain ϵ_i (μ in/in)	ϵ_o (μ in/in)	Inner Radius After Cut (in)
1292-01	3.006	0.310	9.7	8.80	8.76	8.68	8.40	639	-570	2.959
1292-02	3.005	0.314	9.6	7.30	7.62	8.25	8.14	-478	413	3.028
1292-03	3.005	0.313	9.6	8.06	8.21	8.05	8.30	-555	509	3.024
1292-04	3.003	0.322	9.3	7.78	8.05	7.40	7.20	294	-287	2.979
1292-05	3.005	0.308	9.8	7.85	8.05	8.38	8.22	410	-384	2.978
1292-06	3.004	0.315	9.5	8.68	8.45	7.57	7.23	723	-687	2.954
1-1A	2.976	0.300	9.9	9.11	8.63	7.63	8.25	1,593	-1,596	2.875
1-2A	2.972	0.310	9.6	9.31	8.96	8.35	7.45	1,857	-1,908(2)	2.857
1-3A	2.974	0.315	9.4	9.20	9.22	9.18	8.90	-226	216	2.988
1-4A	2.970	0.326	9.1	9.13	9.11	9.08	8.96	-144	134	2.978
1-5A	2.967	0.308	9.6	9.22	9.05	8.78	8.42	1,289	-1,270	2.888
1-6A	2.968	0.289	10.3	8.61	8.79	8.74	8.56	-2,048	1,939	3.111

(1) Determined by resin burnoff.
(2) Gage drifted.

Comparisons with the Curved-Beam Theory

The curved-beam equations for a nonuniform distribution of fibers in the radial direction depend only on the variation of the circumferential modulus of elasticity. The results in Table 4 are based on the data in Table 3 and Equation 52, Page 21.

It is noted in Table 4 that the results achieved in the 1-XA series of rings are very much better than the results of the 1292-XX series. The 1292-XX series of rings were tested about a year ago, and it is uncertain why these results should be so far off. The 1-XA series rings, which were tested recently, apparently provide more reliable data. Consequently, further comparisons are made only with the 1-XA series parts.

It is also apparent that the strain-gage method is superior to the diameter-change method when the elastic modulus variation is accounted for.

For many cases, sufficient accuracy is achieved from the assumption of uniform fiber distribution in the radial direction. With the curved-beam theory, this assumption yields the important advantage of not having to determine the modulus of elasticity. A comparison of the curved-beam theory for uniform material with the experimental data for the -A series of rings is given in Table 5.

Table 4

VARIATION IN E_θ TAKEN INTO ACCOUNT BY MEANS OF THE CURVED-BEAM THEORY

Experimental Results			Curved-Beam Theory					
			Based on Diameter Change				Based on Strain Gage	
Ring Number	ϵ_i (μ in/in)	ϵ_o (μ in/in)	ϵ_i (μ in/in)	Percent Difference	ϵ_o (μ in/in)	Percent Difference	ϵ_o (μ in/in)	Percent Difference
1292-01	639	-570	793.0	24.1	-742.8	30.3	-598.1	4.81
1292-02	-478	413	-384.6	19.5	359.9	12.8	447.4	7.99
1292-03	-555	509	-315.2	43.2	295.1	42.0	519.5	2.04
1292-04	294	-287	429.8	46.1	-401.6	39.9	-274.9	4.31
1292-05	410	-384	459.9	12.1	-431.1	12.2	-384.2	0.05
1292-06	723	-687	866.5	19.8	-810.7	18.0	-676.5	1.54
		Average		27.4		26.0		3.46
1-1A	1,593	-1,596	1,637.8	2.8	-1,620.1	1.5	-1,575.8	1.3
1-2A	1,857	-1,908	1,886.4	1.5	-1,930.8	1.2	-1,900.8	0.4
1-3A	-226	216	-243.6	7.8	230.6	6.7	213.9	0.9
1-4A	-144	134	-144.8	0.6	135.9	1.4	135.2	0.9
1-5A	1,289	-1,270	1,326.0	2.9	-1,287.8	1.4	-1,251.8	1.4
1-6A	-2,048	1,939	-2,307.3	12.6	2,172.6	12.0	1,928.4	0.5
		Average		4.7		3.8		0.7

Note in Table 5 that the efficacy of the diameter-change method compares favorably with the strain-gage method. A comparison of Tables 4 and 5 is also favorable. Apparently, only a slight improvement results from taking the nonuniformity of the fiber distribution into account, and this improvement is only apparent when the strain-gage method is used.

Table 5

COMPARISON OF EXPERIMENTAL DATA OBTAINED BY THE DIAMETER-CHANGE AND STRAIN-GAGE READINGS WHERE A UNIFORM DISTRIBUTION OF FIBERS IS ASSUMED

Experimental Results			Curved-Beam Theory					
			Based on Diameter Change				Based on Strain Gage	
Ring Number	ϵ_i (μ in/in)	ϵ_o (μ in/in)	ϵ_i (μ in/in)	Percent Difference	ϵ_o (μ in/in)	Percent Difference	ϵ_o (μ in/in)	Percent Difference
1-1A	1,593	-1,596	1,683.6	5.69	-1,578.4	1.10	-1,493.5	6.42
1-2A	1,857	-1,908	1,976.3	6.42	-1,849.3	3.08	-1,737.7	8.93
1-3A	-226	216	-245.2	8.50	229.2	6.11	211.3	2.18
1-4A	-144	134	-145.3	0.90	135.5	1.01	134.3	0.22
1-5A	1,289	-1,270	1,351.3	4.83	-1,264.9	0.05	-1,206.6	4.99
1-6A	-2,048	1,939	-2,309.8	12.78	2,170.3	11.93	1,924.2	0.76
		Average		6.52		3.88		3.91

Comparisons with the Elasticity Theory

The elasticity solution is a function of the radial and circumferential components of the elastic modulus and of the Poisson's ratio. The comparisons between the elasticity solutions and the experimental data for the 1-XA series are given in Table 6.

Again, there is some improvement by considering the material to be nonuniform. Also, the diameter-change method is slightly less accurate than the strain-gage method. This difference is probably attributable to the accuracy of measuring the diameters on rings which are somewhat flexible and which have some unevenness in the surface finish.

As expected, the results obtained from the elasticity theory are closely in agreement with the curved-beam theory. Hence, the extra experimental effort that may be necessary to determine all elastic properties may not be entirely justified. For rings of the type here, the results from the simplest method (curved-beam theory for uniform material based on diameter change) are very satisfactory (6.52 and 3.88 average percentage difference with experimental data). The best results are obtained from the strain-gage method where non-uniform material is considered, but the extra experimental work involved probably doesn't justify the increased accuracy.

CONCLUSIONS

The analysis and control of residual stresses is important when using composite materials in applications where optimum performance is desired.

For dealing with a particular material test specimen (the filament-wound ring), two theories and two experimental techniques have been developed here. Of the two theories, the curved-beam method is the simpler to apply, but the elasticity theory has a broader range of application. It is also noted that the curved-beam theory may be applied without knowledge of the elastic properties of the composite material if it is assumed that there is no radial variation of the modulus of elasticity.

Of the two experimental methods, the diameter-change method is thought to be more convenient because of the possible inconvenience of mounting strain gages. However, strain gaging seems to have greater sensitivity, and thus is recommended when more precise results are needed.

Both theoretical methods allow the radial variation of the elastic properties, an important advantage in that rings made of varied materials may be analyzed.

Table 6

COMPARISON OF EXPERIMENTAL RESULTS WITH ELASTICITY THEORY

Ring Number	Experimental Results		Uniform Material Assumed						Nonuniform Material Taken Into Account					
			Based on Diameter Change				Based on Strain Gage		Based on Diameter Change				Based on Strain Gage	
	ϵ_i (μ in/in)	ϵ_o (μ in/in)	ϵ_i (μ in/in)	Percent Difference	ϵ_o (μ in/in)	Percent Difference	ϵ_o (μ in/in)	Percent Difference	ϵ_i (μ in/in)	Percent Difference	ϵ_o (μ in/in)	Percent Difference	ϵ_o (μ in/in)	Percent Difference
1-1A	1,593	-1,596	1,678.7	5.37	-1,574.7	1.33	1,494.3	6.37	1,631.8	2.43	-1,615.6	1.23	-1,577.3	1.17
1-2A	1,857	-1,908	1,970.6	6.11	-1,844.6	3.32	-1,738.0	8.91	1,879.4	1.21	-1,924.8	0.88	-1,901.5	0.34
1-3A	-226	216	-244.5	7.56	228.6	5.83	211.3	2.17	-242.9	7.47	230.0	6.48	214.0	0.93
1-4A	-144	134	-160.4	11.3	148.6	10.89	133.4	0.44	-144.3	0.21	135.6	1.19	135.4	1.04
1-5A	1,289	-1,270	1,347.5	4.53	-1,261.7	0.65	-1,206.8	4.97	1,321.3	2.51	-1,284.4	1.13	-1,253.0	1.33
1-6A	-2,048	1,939	-2,303.8	12.49	2,165.5	11.68	1,925.0	0.72	-2,299.5	12.28	2,168.0	11.8	1,930.2	0.45
		Average		7.89		5.62		3.93		4.35		3.78		0.87

For example, the theory could routinely handle the residual strain distribution in a composite structure consisting of a metal ring covered with fiber glass-epoxy winding; which, in turn, is covered with metal-epoxy winding.

The method of cutting the ring shares the disadvantage with Olson and Bert's method[3] of being a destructive test. However, the amount of labor in the present method is considerably less than that involved in boring out the test specimens. It is felt that a possible improvement could be made in devising a nondestructive test whereby the behavior of a ring compressed between two parallel planes could be indicative of the residual stress. Another nondestructive test could be based on the photoelastic method. This method, in particular, may be useful in leading to a more basic understanding of the mechanism of residual stress in composite materials.

REFERENCES

(1) Mesnager, M.; "Methods de Determination des Tensions Existent dans un Cylindre Circulaire", Comptes Rendus, 169, pp 1391-1393 (1919).

(2) Sachs, G.; "Dev Nachweiss Innerer Spannungen in Stangen and Rohren", Zeitschrift fur Metallkinde, 19, pp 352-357 (1927). The Determination of Residual Stresses in Rods and Tubes; Brutcher Translation Number 1386.

(3) Olson, W. A. and Bert, C. W.; "Analysis of Residual Stresses in Bars and Tubes of Cylindrically Orthotropic Materials", Experimental Mechanics, pp 451-457 (1966).

(4) Fourney, W. L.; "Residual Strain in Filament-Wound Rings (Note)", Journal of Composite Materials, 2, pp 408-411 (1968).

(5) Lekhnitskii, S. G.; Anisotropic Plates; Translated from the Second Russian Edition by S. W. Tsai and T. Cheron; Gordon and Breach, New York (1968).

(6) Timoshenko, S. and Goodier, J. N.; Theory of Elasticity, Second Edition; McGraw-Hill, New York (1951).

(7) Murphy, Glenn; Advanced Mechanics of Materials; McGraw-Hill, New York (1946).

THIS PAGE

WAS INTENTIONALLY

LEFT BLANK

APPENDIX

FORTRAN PROGRAM

Residual Strain Distribution in Filament-Wound Rings - Elasticity Theory for Uniform Material Only

This program is used to compute the residual strain distribution in filament-wound rings by means of the elasticity equations, Page 9. This program is limited to rings where the elastic properties are uniform throughout; when there is a nonuniform distribution, the FORTRAN program that follows applies (Page 37).

Input: (One card for each ring. No limit on the number of cases.)

1-10 Original inside diameter of ring (F format).

11-20 Thickness of ring (F format).

21-30 Tangential modulus, E (F format).

31-40 Radial modulus, E' (F format).

41-50 Reading of the inner strain gage in microinches per inch (F format). If strain gage reading is not furnished, leave blank.

51-60 Inside diameter of the ring after cutting (F format). If the diameter after cutting is not measured, leave blank. If both the diameter and strain-gage readings are available, separate outputs will be given.

Output:

INSIDE RADIUS	original inner radius
THICKNESS	(same as input)
K	ratio E/E'
INNER STRAIN	residual strain on inside surface, microinches/inch
OUTER STRAIN	residual strain on outer surface, microinches/inch

C1	Constant A (Page 12)
C2	Constant B (Page 12)
C3	Constant C (Page 12)

FORTRAN Listing:

```
C     RESIDUAL STRAIN DISTRIBUTION IN FILAMENT WOUND RINGS
C     ELASTICITY THEORY
C     UNIFORM MATERIAL ONLY
C    B.R.D, 11-5-68
     1 WRITE (51,2)
     2 FORMAT (1H1,4X,6HINSIDE,4X,6HTHICK-,6X,1HK,7X,5HINNER,4X,5HOUTER)
     3 WRITE (51,4)
     4 FORMAT (5X,6HRADIUS,5X,4HNESS,15X,6HSTRAIN,3X,6HSTRAIN,9X,2HC1,13X
      1,2HC2,13X,2HC3)
     5 READ (50,6) DI,T,ET,ER,SI,DCUT
     6 FORMAT(6F10.0)
     7 FK = SQRT(ET/ER)
       RI = DI/2.
       RO = RI+T
       RIC = DCUT/2.
       IF (SI) 10,30,10
    10 BOT = 1.0 - FK*(RO**(FK-1.0)*RI**(-FK-1.0) - 2.0/RI**2 + RO**(-FK
      1-1.0)*RI**(FK-1.0) ) / (RI**(FK-1.0)*RO**(-FK-1.0) - RO**(FK-1.0)
      2*RI**(-FK-1.0) )
    11 C1 =  ET*SI/BOT
    12 C2 = C1*(RO**(FK-1.0)-RI**(FK-1.0)) /.(RI**(FK-1.0)*RO**(-FK-1.0)
      1-RO**(FK-1.0)*RI**(-FK-1.0) )
    13 C3 = - C1*(RO**(-FK-1.0)- RI**(-FK-1.0)) / (RI**(FK-1.0)*RO**(-FK
      1-1.0) - RO**(FK-1.0)*RI**(-FK-1.0) )
    14 SO = ( C1 - C2*FK*RO**(-FK-1.0) + C3*FK*RO**(FK-1.0)) / ET
    15 SI = ( C1 - C2*FK*RI**(-FK-1.0) + C3*FK*RI**(FK-1.0)) / ET
    16 WRITE(51,17) RI,T,FK,SI,SO,C1,C2,C3
    17 FORMAT (1H0,3F10.4,2F10.1,3E15.4,10H GAGE DATA)
    30 IF(DCUT) 31,38,31
    31 C1 = (RIC - RI) / (RI*(1.0/ET -1.0/ER))
    32 C2 = C1*(RO**(FK-1.0)-RI**(FK-1.0)) / (RI**(FK-1.0)*RO**(-FK-1.0)
      1-RO**(FK-1.0)*RI**(-FK-1.0))
    33 C3 = - C1*(RO**(-FK-1.0)-RI**(-FK-1.0))/ (RI**(FK-1.0)*RO**(-FK-
      11.0) - RO**(FK-1.0)*RI**(-FK-1.0))
    34 SO = ( C1 - C2*FK*RO**(-FK-1.0) + C3*FK*RO**(FK-1.0)) / ET*1.0E6
    35 SI = ( C1 - C2*FK*RI**(-FK-1.0) + C3*FK*RI**(FK-1.0)) / ET*1.0E6
    36 WRITE (51,37) RI,T,FK,SI,SO,C1,C2,C3,RIC
    37 FORMAT (1H0,3F10.4,2F10.1,3E15.4,17H IR AFTER CUT WAS,F8.4,4H IN.)
    38 WRITE(51,39)
    39 FORMAT (1H0)
    40 GO TO 5
       END
```

Residual Strain Distribution in Filament-Wound Rings - Elasticity Theory for Uniform and Nonuniform Material

This program is used to compute the residual strain in filament-wound rings by means of the elasticity equations (Page 14). This program runs one-layer and four-layer rings; a simple modification is necessary to run any other number of layers.

Input: (One initial card for each ring, plus one additional card for each layer. The groups may be repeated indefinitely.)

Initial Card:

Initial Card:	1-10	Inside diameter (F format).
	11-20	Thickness (F format).
	21-30	Strain reading, microinches per inch (F format). May be left blank.
	31-40	Inside diameter after cutting (F format). May be left blank.
	41	Number of layers, either 1 or 4 (I format).

Additional card for one-layer ring only:

1-10	Tangential modulus, E (E format).
11-20	Radial modulus, E' (E format).
21-30	Poisson's ratio, ν (F format).

Additional cards for four-layer ring only:

1-10	Inside radius of layer, a_i (F format).
11-20	Tangential modulus, E_i (E format).
21-30	Radial modulus, E_i (E format).
31-40	Poisson's ratio, ν_i (F format).

Output:

INSIDE RADIUS	original inner radius
THICKNESS	same as input
INNER STRAIN	computed residual strain on inner fiber, microinches/inch
OUTER STRAIN	computed residual strain on outer fiber, microinches/inch
ALPHA	size of gap in cut rings, radians

Constants A, B, and C for each layer. Under the list of constants is given the source of input for that particular case.

FORTRAN Listing:

```
C      RESIDUAL STRAIN DISTRIBUTION IN FILAMENT WOUND RINGS
C     ELASTICITY THEORY
C      UNIFORM AND NONUNIFORM MATERIAL
C      B.R. DEWEY.    11-5-68.    REVISED 1-10-69
C
       DIMENSION R(5),ET(4),ER(4),GN(4),FK(4),RS(4),A(4),B(4),C(4),F(12),
      1D(12,12),DD(144),SI(4),SO(4)
     1 WRITE (51,2)
       IDEX = 0
     2 FORMAT (1H1,4X,6HINSIDE,4X,6HTHICK-,4X,5HINNER,4X,5HOUTER/ 5X,
      16HRADIUS,5X,4HNESS,5X,6HSTRAIN,3X,6HSTRAIN,5X,5HALPHA///)
C IN STATEMENT 5, NO MUST BE EITHER 1 OR 4.
     5 READ (50,6) DI,T,SA,DCUT,NO
     6 FORMAT (4F10.0,I1)
       RI = DI/2.
       RC = DCUT/2.
       RO =(DI+2.0*T)/2.
     8 IF(NO.NE.1) GO TO 100
C
C   BRANCH FOR HOMOGENEOUS RING--DIAMETER MEASUREMENT
C
    10 READ (50,12) ETAN,ERAD,GNUT
    12 FORMAT (3E10.0)
    14 HK=SQRT(ETAN/ERAD)
       IF(DCUT) 30,30,17
    17 AC = (RC-RI)/ (RI*(1./ETAN - 1./ERAD))
    18 BC = AC*(RC**(HK-1.0)-RI**(HK-1.0))/ (RI**(HK-1.0)*RO**(-HK-1.0) -
      1RO**(HK-1.0)*RI**(-HK-1.0))
    19 CC = AC*(RI**(-HK-1.0) - RO**(-HK-1.0))/(RI**(HK-1.0)*RO**(-HK-1.0
      1) - RO**(HK-1.0)*RI**(-HK-1.0))
       WRITE (51,1001) AC,BC,CC
  1001 FORMAT (60X, 3E15.4)
    20 STRI =  (AC - BC*HK*RI**(-HK-1.0) + CC*HK*RI**(HK-1.0))*1.0E6/ETAN
    21 STRO =  (AC - BC*HK*RO**(-HK-1.0) + CC*HK*RO**(HK-1.0))*1.0E6/ETAN
    22 ALPHA = 6.2832*AC*(1.0/ETAN -1.0/ERAD)
    24 WRITE (51,25) RI,T,STRI,STRO,ALPHA
    25 FORMAT (2F10.4,2F10.1,F10.5,5X,33HDIAMETER MEASUREMENT--HOMOGENEOU
      1S//)
    30 IF (SA) 31,299,31
```

```
C
C   BRANCH FOR HOMOGENEOUS RING--STRAIN MEASURED ON INSIDE SURFACE
C
   31 BOTT = 1.0-HK*(RO**(HK-1.0)*RI**(-HK-1.0)-2.0/RI**2 + RO**(-HK-1.0
     1)*RI**(HK-1.0)) / (RI**(HK-1.0)*RO**(-HK-1.0) - RO**(HK-1.0)* RI**
     2(-HK-1.0))
   32 AC = ETAN*SA/BOTT
   33 BC = AC*(RO**(HK-1.0)-RI**(HK-1.0)) / (RI**(HK-1.0)*RO**(-HK-1.0)
     1-RO**(HK-1.0)*RI**(-HK-1.0))
   34 CC = -AC*(RO**(-HK-1.0)-RI**(-HK-1.0))/(RI**(HK-1.0)*RO**(-HK-1.0)
     1-RO**(HK-1.0)*RI**(-HK-1.0))
      WRITE (51,1001) AC,BC,CC
   35 STRI = (AC - BC*HK*RI**(-HK-1.0)+CC*HK*RI**(HK-1.0))/ETAN
   36 STRO = (AC - BC*HK*RO**(-HK-1.0)+CC*HK*RO**(HK-1.0))/ETAN
   38 WRITE(51,39) RI,T,STRI,STRO
   39 FORMAT (2F10.4,2F10.1/15X,29HSTRAIN GAGE DATA--HOMOGENEOUS///)
   40 GO TO 299
C
C   BRANCH FOR NONHOMOGENEOUS RING--DIAMETER MEASUREMENT
C
  100 IF (NO.NE.4) GO TO 310
      READ (50,101) (R(J),ET(J),ER(J),GN(J),J=1,4)
  101 FORMAT (F10.0,2E10.0,F10.0)
      RO= R(1)+T
      R(5)= RO
  102 DO 104 J=1,4
      FK(J) = SQRT(ET(J)/ER(J))
      RS(J) = DCUT/2. +R(J)-R(1)
  104 CONTINUE
      IF (DCUT)  105,200,105
  105 DO 109 I=1,12
  106 F(I) = 0.0
      DO 109 J=1,12
  109 D(I,J)= 0.0
C     FIRST ROW--GAP SIZE
CHANGE SIGN 110 INSTEAD OF 111  R - R*
  110 D(1,1) = -1.
  111 F(1) = (R(1)-RS(1))/(R(1)*(1.0/ET(1)-1.0/ER(1)))
C     SECOND ROW -- SIGMA R = 0  ON INSIDE
  119 D(2,1) = 1.0
  120 D(2,2) = R(1)**(-FK(1)-1.0)
  121 D(2,3) = R(1)**(FK(1)-1.0)
      DO 149 I=1,3
C     MATCH SIGMA R
  125 D(3*I,  3*I-2) = 1.0
  126 D(3*I,  3*I-1) = R(I+1)**(-FK(I)-1.0)
  127 D(3*I,  3*I  ) = R(I+1)**( FK(I)-1.0)
  128 D(3*I,  3*I+1) = -1.0
  129 D(3*I,  3*I+2) = -R(I+1)**(-FK(I+1)-1.0)
  130 D(3*I,  3*I+3) = -R(I+1)**( FK(I+1)-1.0)
C     MATCH RADIAL DISPLACEMENT U
  131 D(3*I+1,3*I-2) = (FK(I)**2-GN(I))*R(I+1)/ ET(I)
  132 D(3*I+1,3*I-1) = -(FK(I)+GN(I))*R(I+1)**(-FK(I)) /ET(I)
  133 D(3*I+1,3*I  ) =  (FK(I)-GN(I))*R(I+1)**( FK(I)) /ET(I)
  134 D(3*I+1,3*I+1) = -(FK(I+1)**2-GN(I+1))*R(I+1)/ET(I+1)
  135 D(3*I+1,3*I+2) =  (FK(I+1)+GN(I+1))*R(I+1)**(-FK(I+1)) /ET(I+1)
  136 D(3*I+1,3*I+3) = -(FK(I+1)-GN(I+1))*R(I+1)**( FK(I+1)) /ET(I+1)
C     MATCH TANGENTIAL DISPLACEMENT V
  141 D(3*I+2,3*I-2) =  1.0/ET(I) - 1.0/ER(I)
  144 D(3*I+2,3*I+1) = -1.0/ET(I+1) + 1.0/ER(I+1)
  149 CONTINUE
C     ROW 12,  SIGMA R = 0 AT OUTSIDE
  151 D(3*NO,3*NO-2) =  1.0
  152 D(3*NO,3*NO-1) =  RO**(-FK(NO)-1.0)
  153 D(3*NO,3*NO  ) =  RO**( FK(NO)-1.0)
C     CHANGE  D(I,J) TO COLUMN DD(II)
      II = 0
      DO 155 J=1,12
      DO 155 I=1,12
```

```
      II=II+1
  155 DD(II) = D(I,J)
  156 CALL SIMQ (DD,F,12,KSIG)
      IF(KSIG.EQ.1) GO TO 320
C
C     SOLUTION IS IN F.  F(1),F(4),F(7),...HAS A(1),A(2),A(3)...
C                        F(2),F(5),F(8),...HAS B(1),B(2),B(3)...
C                        F(3),F(6),F(9),...HAS C(1),C(2),C(3)...  ETC.
C
  160 DO 165  J=1,4
      A(J) = F(3*J-2)
      B(J) = F(3*J-1)
  165 C(J) = F(3*J   )
C
C  COMPUTE TANGENTIAL STRAIN DISTRIBUTION
C
      DO 168 J=1,4
      WRITE (51,1001) A(J),B(J),C(J)
  167 SI(J) =  (A(J)- B(J)*FK(J)*R(J)**(-FK(J)-1.0) + C(J)*FK(J)*R(J)**
     1(FK(J)-1.0)) / ET(J)*1.0E6
  168 SO(J) =  (A(J)- B(J)*FK(J)*R(J+1)**(-FK(J)-1.0) + C(J)*FK(J)*R(J+1
     1)**(FK(J)-1.0)) / ET(J) *1.0E6
  170 ALPHA = (1.0/ET(1) -1.0/ER(1))*6.2832 *A(1)
      WRITE (51,174)  R(1),T,SI(1),SO(1),ALPHA
  174 FORMAT (1H0,F9.4,F10.4,2F10.1,F10.5,5X,47HDIAMETER MEASUREMENT--NO
     1NHOMOGENEOUS, 4 LAYERS   )
      DO 179 J=2,4
  179 WRITE (51,181)  R(J),SI(J),SO(J)
  181 FORMAT (F10.4,10X,2F10.1)
  183 WRITE (51,184)
  184 FORMAT (1H0///)
      IDEX = IDEX + 5
C
C  BRANCH FOR NONHOMOGENEOUS RING--STRAIN MEASURED ON INSIDE SURFACE
C
  200 IF (SA) 201,299,201
  201 DO 205 I= 1,12
  203 F(I)= 0.0
      DO 205 J=1,12
  205 D(I,J)= 0.0
      F(1) = SA*1.0E-6
C
COEFFICIENTS--COLUMN 1,4,7,10--A,  2,5,8,11--B.  3,6,9,12--C.
C     FIRST ROW -- STRAIN READING
  211 D(1,1) = 1.0/ET(1)
  212 D(1,2) =-FK(1)*R(1)**(-FK(1)-1.0)/ET(1)
  213 D(1,3) = FK(1)*R(1)**(FK(1)-1.0)/ET(1)
C     SECOND ROW -- SIGMA R = 0 ON INSIDE
  221 D(2,1) = 1.0
     1/1.0E6
  222 D(2,2) = R(1)**(-FK(1)-1.0)
     1/1.0E6
  223 D(2,3) = R(1)**(FK(1)-1.0)
     1/1.0E6
C     INSIDE ROWS  MATCH  SIGMA R, U, V AT THE INTERFACE
      DO 259 I=1,3
C   MATCH SIGMA R
  231 D(3*I,  3*I-2) = 1.0
     1/1.0E6
  232 D(3*I,  3*I-1) = R(I+1)**(-FK(I)-1.0)
     1/1.0E6
  233 D(3*I,  3*I   ) = R(I+1)**(FK(I)-1.0)
     1/1.0E6
  234 D(3*I,  3*I+1) = -1.0
     1/1.0E6
  235 D(3*I,  3*I+2) = -R(I+1)**(-FK(I+1)-1.0)
     1/1.0E6
  236 D(3*I,  3*I+3) = -R(I+1)**(FK(I+1)-1.0)
     1/1.0E6
```

```
C   MATCH U
 241 D(3*I+1,3*I-2) =  (FK(I)**2-GN(I))*R(I+1) /ET(I)
 242 D(3*I+1,3*I-1) = -(FK(I)+GN(I))*R(I+1)**(-FK(I))/ET(I)
 243 D(3*I+1,3*I  ) =  (FK(I)-GN(I))*R(I+1)**(FK(I)) /ET(I)
 244 D(3*I+1,3*I+1) = -(FK(I+1)**2-GN(I+1))*R(I+1)/ET(I+1)
 245 D(3*I+1,3*I+2) =  (FK(I+1)+GN(I+1))*R(I+1)**(-FK(I+1))/ET(I+1)
 246 D(3*I+1,3*I+3) = -(FK(I+1)-GN(I+1))*R(I+1)**( FK(I+1))/ET(I+1)
C   MATCH V
 251 D(3*I+2,3*I-2) =  1.0/ET(I) -1.0/ER(I)
 254 D(3*I+2,3*I+1) = -1.0/ET(I+1) + 1.0/ER(I+1)
 259 CONTINUE
C    LAST ROW, SIGMA R = 0 AT OUTSIDE
 260 D(3*NO,3*NC-2) =  1.0
    1/1.0E6
 261 D(3*NO,3*NC-1) = RO**(-FK(NO)-1.0)
    1/1.0E6
 262 D(3*NO,3*NC  ) = RO**(FK(NO)-1.0)
    1/1.0E6
C  PLACE ARRAY D(I,J) INTO COLUMN FORM DD(II)
     II= 0
     DO 265  J=1,12
     DO 265  I=1,12
     II=II+1
 265 DD(II) = D(I,J)
 266 CALL SIMQ (DD,F,12,KSIG)
     IF(KSIG.EQ.1) GO TO 330
 270 DO 275 I=1,4
     A(I) = F(3*I-2)
     B(I) = F(3*I-1)
 275 C(I) = F(3*I)
C  STRAIN DISTRIBUTION
     DO 280 J=1,4
     WRITE (51,1001) A(J),B(J),C(J)
 278 SI(J) = (A(J)-B(J)*FK(J)*R(J)**(-FK(J)-1.0)+C(J)*FK(J)*R(J)**(FK(J
    1)-1.0))/ET(J) * 1.0E6
 280 SO(J) = (A(J)-B(J)*FK(J)*R(J+1)**(-FK(J)-1.0) + C(J)*FK(J)*R(J+1)
    1**(FK(J)-1.0)) / ET(J) * 1.0E6
 281 ALPHA = (1.0/ET(1) - 1.0/ER(1))*6.2832*A(1)
     WRITE (51,284) R(1),T,SI(1),SO(1),ALPHA
 284 FORMAT (1H0,F9.4,F10.4,2F10.1,F10.5,5X,45HSTRAIN MEASUREMENT--NONH
    1OMOGENEOUS, 4 LAYERS   )
     DO 286 J=2,4
 286 WRITE (51,288) R(J),SI(J),SO(J)
 288 FORMAT (F10.4,10X,2F10.1)
 290 WRITE (51,184)
     IDEX = IDEX + 5
 299 IDEX = IDEX + 1
 300 IF (IDEX-25) 5,1,1
 310 WRITE(51,311)
 311 FORMAT(1H0,47HSORRY, THIS PROGRAM ONLY WORKS FOR FOUR LAYERS.)
     GO TO 299
 320 WRITE(51,312)
 312 FORMAT(1H0,42HSUBROUTINE SIMQ REPORTS SINGULAR EQUATIONS)
     GO TO 200
 330 WRITE(51,312)
     GO TO 299
     END
C     THIS IS ORNL F04001 OF 1167
C     ...............................................................
C
C        SUBROUTINE SIMQ
C
C        PURPOSE
C           OBTAIN SOLUTION OF A SET OF SIMULTANEOUS LINEAR EQUATIONS,
C           AX=B
C
C        USAGE
C           CALL SIMQ(A,B,N,KS)
C
```

```
C        DESCRIPTION OF PARAMETERS
C           A - MATRIX OF COEFFICIENTS STORED COLUMNWISE.  THESE ARE
C               DESTROYED IN THE COMPUTATION.  THE SIZE OF MATRIX A IS
C               N BY N.
C           B - VECTOR OF ORIGINAL CONSTANTS (LENGTH N). THESE ARE
C               REPLACED BY FINAL SOLUTION VALUES, VECTOR X.
C           N - NUMBER OF EQUATIONS AND VARIABLES
C           KS - OUTPUT DIGIT
C                0 FOR A NORMAL SOLUTION
C                1 FOR A SINGULAR SET OF EQUATIONS
C
C        REMARKS
C           MATRIX A MUST BE GENERAL.
C           IF MATRIX IS SINGULAR , SOLUTION VALUES ARE MEANINGLESS.
C           AN ALTERNATIVE SOLUTION MAY BE OBTAINED BY USING MATRIX
C           INVERSION (MINV) AND MATRIX PRODUCT (GMPRD).
C
C        SUBROUTINES AND FUNCTION SUBPROGRAMS REQUIRED
C           NONE
C
C        METHOD
C           METHOD OF SOLUTION IS BY ELIMINATION USING LARGEST PIVOTAL
C           DIVISOR. EACH STAGE OF ELIMINATION CONSISTS OF INTERCHANGING
C           ROWS WHEN NECESSARY TO AVOID DIVISION BY ZERO OR SMALL
C           ELEMENTS.
C           THE FORWARD SOLUTION TO OBTAIN VARIABLE N IS DONE IN
C           N STAGES. THE BACK SOLUTION FOR THE OTHER VARIABLES IS
C           CALCULATED BY SUCCESSIVE SUBSTITUTIONS. FINAL SOLUTION
C           VALUES ARE DEVELOPED IN VECTOR B, WITH VARIABLE 1 IN B(1),
C           VARIABLE 2 IN B(2),........, VARIABLE N IN B(N).
C           IF NO PIVOT CAN BE FOUND EXCEEDING A TOLERANCE OF 0.0,
C           THE MATRIX IS CONSIDERED SINGULAR AND KS IS SET TO 1. THIS
C           TOLERANCE CAN BE MODIFIED BY REPLACING THE FIRST STATEMENT.
C
C     ..................................................................
C
      SUBROUTINE SIMQ(A,B,N,KS)
      DIMENSION A(144), B(12)
C
C        FORWARD SOLUTION
C
      TOL=0.0
      KS=0
      JJ=-N
      DO 65 J=1,N
      JY=J+1
      JJ=JJ+N+1
      BIGA=0
      IT=JJ-J
      DO 30 I=J,N
C
C        SEARCH FOR MAXIMUM COEFFICIENT IN COLUMN
C
      IJ=IT+I
      IF(ABS(BIGA)-ABS(A(IJ))) 20,30,30
   20 BIGA=A(IJ)
      IMAX=I
   30 CONTINUE
C
C        TEST FOR PIVOT LESS THAN TOLERANCE (SINGULAR MATRIX)
C
      IF(ABS(BIGA)-TOL) 35,35,40
   35 KS=1
      RETURN
C
C        INTERCHANGE ROWS IF NECESSARY
C
   40 I1=J+N*(J-2)
      IT=IMAX-J
```

```
      DO 50 K=J,N
      I1=I1+N
      I2=I1+IT
      SAVE=A(I1)
      A(I1)=A(I2)
      A(I2)=SAVE
C
C        DIVIDE EQUATION BY LEADING COEFFICIENT
C
   50 A(I1)=A(I1)/BIGA
      SAVE=B(IMAX)
      B(IMAX)=B(J)
      B(J)=SAVE/BIGA
C
C        ELIMINATE NEXT VARIABLE
C
      IF(J-N) 55,70,55
   55 IQS=N*(J-1)
      DO 65 IX=JY,N
      IXJ=IQS+IX
      IT=J-IX
      DO 60 JX=JY,N
      IXJX=N*(JX-1)+IX
      JJX=IXJX+IT
   60 A(IXJX)=A(IXJX)-(A(IXJ)*A(JJX))
   65 B(IX)=B(IX)-(B(J)*A(IXJ))
C
C        BACK SOLUTION
C
   70 NY=N-1
      IT=N*N
      DO 80 J=1,NY
      IA=IT-J
      IB=N-J
      IC=N
      DO 80 K=1,J
      B(IB)=B(IB)-A(IA)*B(IC)
      IA=IA-N
   80 IC=IC-1
      RETURN
      END
```

Residual Strain Distribution in Filament-Wound Rings - Strain Distribution by the Curved-Beam Theory for Uniform and Nonuniform Material

This program utilizes the equations of the curved-beam theory (Page 19) to compute the residual strain distribution in rings where there is either a uniform or nonuniform distribution of fibers in the radial direction. Minor modification is required if other than one or four-layered rings are to be analyzed.

Input: (One initial card for each ring. If the modulus of elasticity varies in the radial direction, there is one additional card for each layer.)

Initial Card:

Initial Card:	1-10	Inside diameter (F format).
	11-20	Thickness (F format).
	21-30	Inner strain reading, microinches per inch (F format.) May be left blank.
	31-40	Inside diameter after cutting (F format). May be left blank.
	41-50	Number of layers, either 1 or 4.

Additional cards for four-layer ring only:

1-10	Modulus of elasticity (F format). Note: the program uses ratios of E; thus, it is usually more convenient to enter E without the 10^6.

Output:

INSIDE RADIUS	original inside radius
THICKNESS	(same as input)
R	location of neutral surface
INNER STRAIN	computed residual strain on inner fiber, microinches/inch
OUTER STRAIN	computed residual strain on outer fiber, microinches/inch
GAP SIZE	computed width of opening of cut ring at $r = a_1$ source of input for computed data

FORTRAN Listing:

```
C     RESIDUAL STRAIN DISTRIBUTION IN FILAMENT WOUND RINGS
C   STRAIN DISTRIBUTION BY CURVED BEAM THEORY
C     UNIFORM AND NONUNIFORM MATERIAL
C     B.R. DEWEY,    10-15-68
      DIMENSION E(4), R(5), ET(4)
      EQUIVALENCE (E(1),ET(1))
    1 WRITE(51,2)
      IDEX = 0
    2 FORMAT (1H1,4X,6HINSIDE,4X,6HTHICK-,6X,1HR,7X,5HINNER,4X,5HOUTER,
     10X,3HGAP)
    3 WRITE(51,4)
    4 FORMAT (5X,6HRADIUS,5X,4HNESS,15X,6HSTRAIN,3X,6HSTRAIN,8X,4HSIZE)
    5 READ(50,6) DI,T,SI,DCUT,NO
    6 FORMAT(4F10.0,I1)
      RI = DI/2
    8 IF(NO-1)20,20,9
    9 TOP = 0.
      BOT = 0.
   10 READ(50,11)(E(J),J=1,4)
   11 FORMAT (4F10.0)
      R(1) = RI
   15 DO 18 J=1,4
      R(J+1) = R(J) + T/4.0
      TOP = TOP + E(J)*T/4.0
   18 BOT = E(J)*ALOG(R(J+1)/R(J))+ BOT
   19 RNA = TOP/BOT
      GO TO 30
C   NEUTRAL SURFACE FOR E = CONSTANT
   20 RNA = T/(ALOG((RI+T)/RI))
   30 IF(SI) 31,40,31
   31 SO =-(RI+T-RNA)/(RNA-RI) * RI/(RI+T)* SI
      WRITE (51,33) RI,T,RNA,SI,SO
   33 FORMAT (1H0,3F10.4,2F10.1,15X,16HFROM STRAIN GAGE)
   40 IF(DCUT)41,50,41
   41 GAP = (DCUT - DI)/2.
      CON= GAP/RI
      SI =-CON*(RNA-RI)/RI *1.0E6
      SO = CON*(RI+T-RNA)/(RI+T)*1.0E6
      WRITE (51,43) RI,T,RNA,SI,SO,GAP
   43 FORMAT (1H0,3F10.4,2F10.1,F10.4,5X,25HFROM DIAMETER MEASUREMENT)
   50 IDEX = IDEX + 1
      IF (IDEX - 28) 5,5,1

      END
```